

Orientation dependency of broad-line widths in quasars and consequences for black-hole mass estimation

Matt J. Jarvis^{1*} and Ross J. McLure^{2†}

¹*Astrophysics, Department of Physics, Keble Road, Oxford, OX 3RH, U.K.*

²*Institute for Astronomy, University of Edinburgh, Royal Observatory, Edinburgh EH9 3HJ, U.K.*

17 May 2007

ABSTRACT

In this paper we report new evidence that measurements of the broad-line widths in quasars are dependent on the source orientation, consistent with the idea that the broad-line region is flattened or disc-like. This reinforces the view derived from radio-selected samples, where the radio-core dominance has been used as a measure of orientation. The results presented here show a highly significant (> 99.95 per cent) correlation between radio spectral index (which we use as a proxy for source orientation) and broad-line width derived from the $H\beta$ and $MgII$ emission lines. This is the first time that this type of study has used quasars derived from a large optically selected quasar sample, where the radio-loud quasars (RLQs) and radio-quiet quasars (RQQs) have indistinguishable distributions in redshift, bolometric luminosity and colour, and therefore overcomes any biases which may be present in only selecting via radio emission.

We find that the mean FWHM for the flat-spectrum ($\alpha_{\text{rad}} \lesssim 0.5$) radio-loud quasars (FSQs) to be $\overline{\text{FWHM}}_{\text{FSQ}} = 4990 \pm 536 \text{ km s}^{-1}$, which differs significant from the mean FWHM of the steep-spectrum ($\alpha_{\text{rad}} > 0.5$) radio-loud quasars (SSQs), where $\overline{\text{FWHM}}_{\text{SSQ}} = 6464 \pm 506 \text{ km s}^{-1}$. We also find that the distribution in FWHM for the FSQs is indistinguishable from that of the radio-quiet quasars (RQQs), where $\overline{\text{FWHM}}_{\text{RQQ}} = 4831 \pm 25 \text{ km s}^{-1}$. Considering other observational results in the literature we interpret this result in the context of a significant fraction of the FSQs being derived from the underlying RQQ population which have their radio flux Doppler boosted above the RLQ/RQQ divide.

Under the assumption of a disc-like broad-line region we find no evidence for a difference in the average line-of-sight angle for RQQs and RLQs, implying that the difference is due to black-hole mass. However, we caution against the virial method to estimate black-hole masses in small or ill-defined quasar samples due to significant orientation dependencies. Disentangling the relative importance of black-hole mass and orientation would require higher resolution radio observations. However, orientation effects could be minimised by obtaining low frequency ($< 1 \text{ GHz}$) radio observations of the optically selected SDSS quasars.

Key words: galaxies:active - galaxies:nuclei - quasars:general - radio continuum:galaxies - quasars:emission lines

1 INTRODUCTION

The orientation dependent unification picture of AGN has now been in place for well over a decade (Barthel 1989; Antonucci 1993) and in particular, measures of source orientation in the radio waveband have played a crucial role in the

development of this picture (Urry & Padovani 1995). Under this unification scheme of radio-loud AGN, we see the sources which have their radio jets pointing along our line-of-sight as flat-radio-spectrum quasars (FSQs), with a radio spectral index $\alpha_{\text{rad}} < 0.5$ ¹. The flat spectrum arises from the

* Email: m.jarvis1@physics.ox.ac.uk

† Email: rjm@roe.ac.uk

¹ We use the definition $S_{\nu} \propto \nu^{-\alpha_{\text{rad}}}$, where S_{ν} is the flux density at frequency ν , and α_{rad} is the radio spectral index

superposition of many relativistically beamed synchrotron self-absorbed spectra. These flat-spectrum sources usually exhibit the optical characteristics of quasars, i.e. they are unresolved in optical imaging observations and have broad permitted emission lines ($\text{FWHM} > 2000 \text{ km s}^{-1}$). High-frequency ($\nu > 1 \text{ GHz}$) radio surveys (e.g. Drinkwater et al. 1997) preferentially pick-out these FSQs due to the fact that their radio emission does not become fainter at high frequencies, as is observed in optically thin synchrotron sources.

Conversely, the other extreme is a source with its radio jets aligned along the plane of the sky. In this case the bulk of the emission arises from the optically thin lobes which can extend up to Mpc scales, and these sources are classified as radio galaxies. The radio spectra of the lobes which dominate the radio spectrum of these sources are predominantly steep with $\alpha_{\text{rad}} > 0.5$. These sources dominate the low-frequency radio surveys, such as the complete samples derived from the 3CRR (Laing, Riley & Longair 1983), 6CE (Eales et al. 1997) 7CRS (Willott et al. 2002) and the Westerbork Northern Sky Survey (WENSS; Rengelink et al. 1997). Optically these sources appear as normal galaxies, usually with some extended line emission in the direction of the radio jets; the so-called alignment effect (e.g. van Breugel, Heckman & Miley 1984; Inskip et al. 2002). The spectra of these objects only contain narrow emission lines ($\text{FWHM} < 2000 \text{ km s}^{-1}$) that are believed to reside beyond the obscuring torus.

Between these two extreme cases, where the jets lie at an angle $\lesssim 45$ degrees (e.g. Barthel 1989) to the line-of-sight we still see broad emission lines and also some emission from the flat-spectrum core, however there is also a large contribution from the large scale, steep-spectrum radio lobes. In this case the total radio spectra are somewhere in between the flat-spectrum core dominated sources and the core-less, lobe-dominated radio galaxies and can thus exhibit both components, these are the steep-spectrum radio-loud quasars (SSQs).

Using this argument, the total radio spectral index is therefore an indicator of the orientation of the source on the sky. This is also reinforced by another orientation estimator based around the same argument. The strength of the core radio emission in quasars, when compared to the extended emission, has been used extensively as an indication of source orientation (e.g. Wills & Browne 1986; Brotherton 1996).

With these measures of orientation which are presented by radio-loud sources we are able to probe the geometry of other properties inherent to powerful quasars. One such property is the geometry of the broad-line region. Thus far, studies of this type have been restricted to radio-selected samples which are difficult to reconcile with the more abundant radio-quiet quasar population. However, with the recent large-scale quasar surveys coupled with all-sky radio surveys, we are now able to construct large samples of both radio-quiet and radio-loud quasars with consistent selection criteria.

In this paper we use a sub-sample of the Sloan Digital Sky Survey quasar catalogue to investigate the dependency of broad-line width on source orientation in a sample of radio-loud quasars. The important difference of this study to previous studies is that the radio-loud sources are selected with exactly the same criteria as the larger popula-

tion of radio-quiet sources in the sample. Thus we are able to directly infer the orientation effects which may present a distorted view of the radio-quiet population. Such an effect may be very important if we are to continue using the broad-line measurements as an important component in determining black-hole masses of quasars, via the virial estimate (e.g. Kaspi et al. 2000; Vestergaard 2002; McLure & Jarvis 2002), over the history of the Universe (e.g. McLure & Dunlop 2004).

The paper is set out as follows, in Section 2 we provide a brief description of the sample of quasars defined by McLure & Jarvis (2004). In section 3 we present evidence for a correlation between broad line width and radio spectral index, and then go on to determine the parameters of a disc-like geometry for the broad-line region in RLQs. In section 4 we attempt to relate the broad-line width distribution in the radio-loud quasars (RLQs) with that of the radio-quiet quasars (RQQs), and outline the implications that this would have in using broad-line widths to estimate black-hole masses. We summarise our results in section 5. All cosmological calculations presented in this paper assume $\Omega_{\text{M}} = 0.3$, $\Omega_{\Lambda} = 0.7$, $H_0 = 70 \text{ km s}^{-1} \text{ Mpc}^{-1}$.

2 THE SAMPLE

For this analysis we use quasars drawn from the full sample of McLure & Jarvis (2004). These were selected from the SDSS quasar catalogue II (SQCII; Schneider et al. 2003). Only those quasars which fell within the SDSS/FIRST overlap region were included². This ensures complete coverage in the radio wave band and both radio-loud and radio-quiet quasars were completely matched in terms of optical luminosity and redshift distributions. Therefore, any biases that could be present due to targeted selection of FIRST (Becker, White & Helfand 1995) radio sources are negated.

For the purposes of this paper we use the definition of radio-loudness of Miller, Peacock & Mead (1990; i.e. $L_{1.4} > 10^{24} \text{ W Hz}^{-1} \text{ sr}^{-1}$), which results in a total sample size of 409. However, to ensure that we have an indicator of orientation through measurement of the radio spectral index, we cross-correlate our sample with the WENSS (Rengelink et al. 1997), and to ensure a matching of spatial resolution also with the NVSS (Condon et al. 1998). Both the NVSS and WENSS have spatial resolutions of $\sim 30 - 40$ arcsec at 325 MHz and 1.4 GHz respectively.

The need for each source to be matched with a source in the WENSS means that the sample size is reduced significantly due to the fact WENSS only covers the sky north of 30 degrees in declination and at a significantly higher flux-density limit of $S_{325} > 18 \text{ mJy}$ (5σ rms). Of the 409 objects in the radio-loud sample, 121 lie in the area covered by the WENSS, 53 of which have flux-densities greater the WENSS flux-density limit.

² We note that using the quasar catalogue from SDSS DR3 does not enhance our data set in any way as there are the same number of radio-loud quasars with our selection criteria.

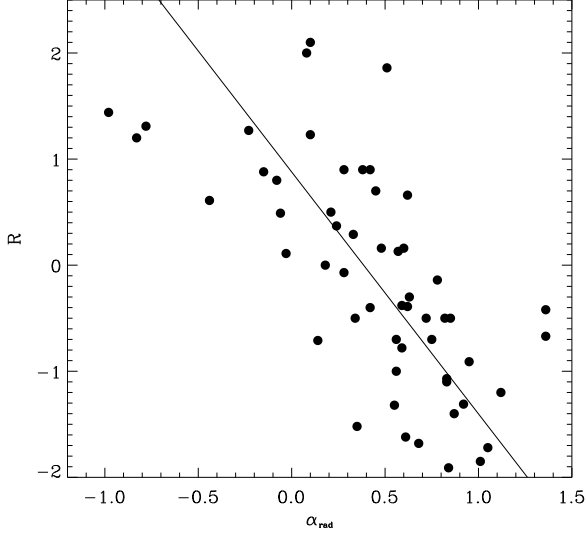


Figure 1. The relation between the radio-core dominance and the radio spectral index from the sample defined by Brotherton (1996). The solid line is the best fit to the data where the fitting takes account of uncertainties in both α_{rad} and R .

3 ORIENTATION DEPENDENCE OF BROAD-EMISSION LINES?

3.1 Radio spectral index as a proxy for source orientation

The radio sources in our sample are derived from the optically selected SDSS quasar catalogue. Therefore in-depth studies have not yet investigated the radio structure of these sources, unlike other widely used radio surveys, such as the 3CRR (Laing et al. 1983). For this reason we are limited in our analysis, due to the fact that we have no morphological constraint on the source orientation. Even the FIRST radio survey does not have enough spatial resolution (the spatial resolution of FIRST is ~ 5 arcsec) to measure the core-to-lobe flux ratio (the R parameter; Hine & Scheuer 1980; Orr & Browne 1982; Hough & Readhead 1989) for the majority of our sample.

However, as previously discussed, many studies in the literature have shown that the radio-spectral index α_{rad} may be a good indicator of the source orientation. This stems from the unification picture of radio-loud AGN and has been confirmed observationally by both Wills & Browne (1986) and Brotherton (1996). Brotherton used a sample 60 radio-loud quasars to investigate the relation between radio-core dominance and broad-line FWHM. In Fig. 1 we plot the radio spectral index and the radio core-dominance parameter R , from Table 1 of Brotherton (1996). This shows a highly significant correlation (> 99.99 per cent) between these two parameters with a dispersion in α_{rad} of $\sigma_{\alpha} = 0.37$ for a given R parameter (and $\sigma_R = 0.87$ for a given α_{rad}). Given that the R parameter has been used extensively to estimate the orientation of radio sources we use α_{rad} as a proxy for R and thus source orientation for the purposes of this study.

Table 1. Radio-loud sources in the sample used in this analysis. All radio luminosities are given in $\text{W Hz}^{-2} \text{ sr}^{-1}$ and the survey from which they are derived are also listed.

| z | α_{rad} | FWHM km s^{-1} | $\log_{10}(L_{325})$ WENSS | $\log_{10}(L_{1.4})$ NVSS | $\log_{10}(L_{1.4})$ FIRST |
|------|-----------------------|----------------------------|-------------------------------|------------------------------|-------------------------------|
| 0.32 | 0.53 | 5333 | 24.03 | 23.51 | 22.72 |
| 0.34 | 0.60 | 3304 | 25.31 | 24.87 | 24.63 |
| 0.34 | 0.90 | 10531 | 25.59 | 24.75 | 23.72 |
| 0.41 | 0.42 | 2554 | 24.49 | 24.20 | 24.12 |
| 0.43 | 0.64 | 1902 | 24.71 | 24.29 | 24.24 |
| 0.45 | 0.77 | 9404 | 25.01 | 24.50 | 24.46 |
| 0.56 | 0.51 | 5695 | 24.85 | 24.44 | 24.22 |
| 0.58 | 0.51 | 5655 | 25.68 | 25.32 | 25.22 |
| 0.59 | 0.23 | 4836 | 26.93 | 26.76 | 26.71 |
| 0.64 | 0.59 | 2549 | 24.62 | 24.29 | 24.37 |
| 0.69 | -0.04 | 2478 | 24.80 | 24.85 | 24.91 |
| 0.70 | 0.60 | 6201 | 25.20 | 24.59 | 24.20 |
| 0.73 | -0.92 | 4082 | 24.57 | 25.02 | 24.81 |
| 0.77 | 0.43 | 5613 | 25.17 | 24.89 | 24.87 |
| 0.79 | 1.26 | 4831 | 24.69 | 24.31 | 24.93 |
| 0.81 | 0.63 | 6491 | 25.77 | 25.10 | 24.71 |
| 0.82 | 0.80 | 4672 | 26.36 | 25.44 | 24.84 |
| 0.84 | 0.34 | 2699 | 25.88 | 25.60 | 25.51 |
| 0.85 | 0.47 | 3545 | 26.05 | 25.69 | 25.60 |
| 0.88 | 0.48 | 7358 | 25.88 | 25.56 | 25.55 |
| 0.89 | 0.85 | 7519 | 25.59 | 24.96 | 24.83 |
| 0.93 | -0.13 | 5001 | 25.43 | 25.47 | 25.42 |
| 1.00 | 0.71 | 5946 | 26.21 | 25.38 | 24.97 |
| 1.02 | -0.35 | 2336 | 24.90 | 25.13 | 25.13 |
| 1.03 | 0.65 | 5854 | 26.15 | 25.22 | 24.68 |
| 1.07 | 1.23 | 8722 | 27.66 | 26.85 | 26.83 |
| 1.14 | 0.49 | 5122 | 25.68 | 25.36 | 25.36 |
| 1.17 | 0.77 | 4986 | 25.84 | 25.11 | 24.90 |
| 1.17 | 0.23 | 3618 | 25.21 | 25.03 | 25.00 |
| 1.32 | 0.45 | 7065 | 27.15 | 26.76 | 26.68 |
| 1.33 | 0.73 | 6496 | 26.64 | 25.97 | 25.82 |
| 1.35 | 0.55 | 4678 | 25.61 | 25.22 | 25.20 |
| 1.39 | 0.43 | 8801 | 25.69 | 25.35 | 25.31 |
| 1.41 | 0.87 | 7020 | 27.05 | 25.86 | 25.43 |
| 1.44 | 0.97 | 15694 | 27.78 | 26.20 | 25.58 |
| 1.44 | 0.22 | 13409 | 26.02 | 25.86 | 25.84 |
| 1.46 | 0.41 | 7165 | 25.97 | 25.63 | 25.59 |
| 1.48 | 0.77 | 6122 | 27.20 | 26.69 | 26.68 |
| 1.55 | -0.18 | 3097 | 25.08 | 25.20 | 25.20 |
| 1.57 | 0.71 | 7898 | 26.73 | 25.92 | 25.73 |
| 1.59 | 1.06 | 9156 | 26.56 | 25.44 | 25.20 |
| 1.63 | 0.21 | 3109 | 25.69 | 25.46 | 25.41 |
| 1.71 | 0.18 | 3366 | 26.71 | 26.52 | 26.49 |
| 1.71 | 0.53 | 5504 | 25.84 | 25.16 | 25.00 |
| 1.72 | 0.30 | 5371 | 25.57 | 25.33 | 25.31 |
| 1.74 | 0.47 | 2848 | 25.89 | 25.64 | 25.66 |
| 1.79 | 0.39 | 2897 | 26.13 | 25.86 | 25.85 |
| 1.80 | 0.87 | 4716 | 28.45 | 26.76 | 26.28 |
| 1.85 | 0.47 | 6462 | 25.71 | 25.36 | 25.34 |
| 1.85 | 0.67 | 8208 | 26.25 | 25.60 | 25.51 |
| 1.91 | 0.94 | 5891 | 27.35 | 26.48 | 26.38 |
| 1.99 | 0.36 | 5473 | 26.72 | 26.41 | 26.38 |
| 2.03 | 0.08 | 6435 | 26.06 | 26.02 | 26.03 |

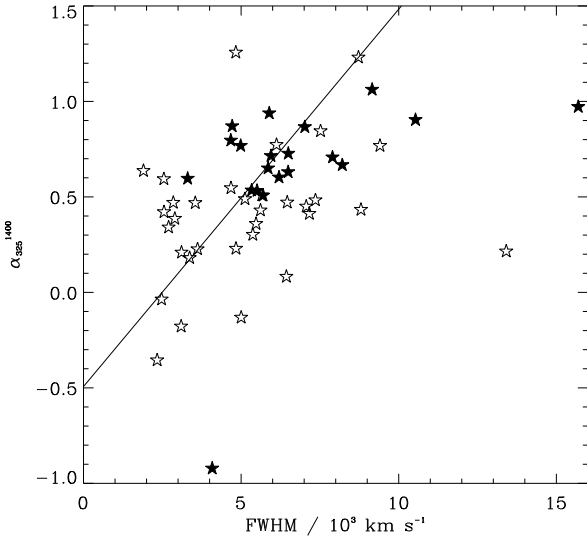


Figure 2. The radio spectral index (measured between 1400 and 325 MHz) versus the measured broad emission-line FWHM for the sample of radio-loud quasars discussed in section 2. The open stars represent those sources where the integrated flux measured from the FIRST catalogue is within a factor of two of the integrated flux measured from the NVSS catalogue. The solid symbols are sources where the ratio of FIRST/NVSS flux-density is less than two, implying that there is a significant extended component. The solid line represents the best fit to the correlation accounting for the uncertainties in both α_{rad} and FWHM. One can immediately see that the detection of extended emission is heavily biased to those sources with steep ($\alpha_{\text{rad}} > 0.5$) spectral index as expected in the orientation-based unification scheme.

3.2 FWHM versus radio spectral index

In Fig. 2 we show the radio spectral index versus the FWHM of the H β or MgII emission lines, depending on the redshift of the source ($0.1 < z < 0.7$ for H β and $0.5 < z < 2.1$ for MgII)³. The sample used here is comprised of all of those sources with a detection in the WENSS catalogue (see Table 1). One can immediately see a correlation between the two parameters. The Spearman rank coefficient for these two parameters is $\rho = 0.459$ with a significance of the correlation being present > 99.95 per cent. Using Kendall's rank we find a similar statistical significance with $\tau = 0.324$ and a significance again of > 99.95 per cent. As these radio sources are selected by exactly the same method i.e. SDSS optical selection and present in the WENSS, with no biases that would influence the measurement of both the FWHM and spectral index, this correlation is undoubtedly real.

Moreover, if we now split the radio-loud sources in this sample into flat-spectrum ($\alpha_{\text{rad}} < 0.5$; FSQs) and steep-spectrum quasars ($\alpha_{\text{rad}} > 0.5$; SSQs), then the difference in the measured FWHM for these two populations is highly significant. The 25 FSQs have a mean and standard error of FWHM = $4990 \pm 536 \text{ km s}^{-1}$, whereas the 28 SSQs have

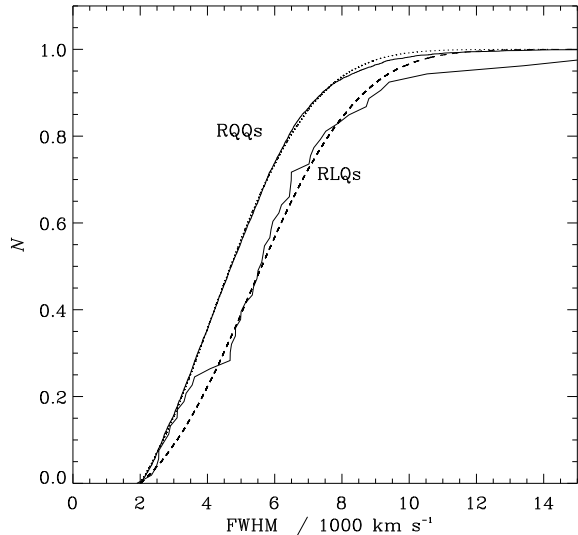


Figure 3. The best-fit models to the cumulative distribution in FWHM for the RQQs (left) and the RLQs (right). The distributions from the data are represented by the solid lines and the models are the dotted (RQQs) and dashed line (RLQs). The best-fit model for the RLQs was obtained by freezing σ_{orb} and θ_{max} at the same values found for the RQQs (see text for details).

a mean FWHM = $6464 \pm 506 \text{ km s}^{-1}$. The KS-test also shows that the distributions in FWHM for FSQs and SSQs are significantly different, with a probability of 4 per cent that they are drawn from the same underlying distribution.

This is in line with previous studies in the literature which have used both the spectral index and the ratio of the core emission to the extended lobe emission to investigate the dependence of broad-line width on source orientation. Using a sample of radio-loud quasars derived from various radio surveys Wills & Browne (1986) found evidence for a significant (> 99.9 per cent) correlation between radio-spectral index and the FWHM of broad emission lines. These authors also compiled the necessary data to investigate the relation between the R parameter and the FWHM. Again they found a significant relation between FWHM and R , and thus source orientation. This can be seen qualitatively in Fig. 2, where only the steep-spectrum sources exhibit an excess of extended emission at the NVSS resolution when compared to the higher resolution FIRST flux-density. The fact that our sample is derived from an optically selected quasar sample provides additional constraints on the link between orientation and radio spectral index, and also a way of probing the distribution in orientation for RQQs.

3.3 Do radio-quiet quasars have orientation dependent broad lines?

The unique way in which our sample is defined means that we are able to directly relate our findings for the radio-loud quasars to the larger radio-quiet quasar (RQQ) population which have been selected from the same optical survey, namely the SDSS. In McLure & Jarvis (2004) we ensured that the radio-quiet and radio-loud quasar samples

³ The method of fitting the broad-line widths to these emission lines is described fully in McLure & Dunlop (2004), where they also show that the FWHM of H β and MgII are consistent for spectra where both are present.

possessed the same distribution in both redshift, bolometric luminosity and photometric colour.

However, the mean FWHMs and standard errors of the RQQs and RLQs from our sample are $4831 \pm 25 \text{ km s}^{-1}$ and $5858 \pm 129 \text{ km s}^{-1}$ respectively. This was predominantly the reason for the difference in the estimates of the black-hole masses for RQQs and RLQs discussed in McLure & Jarvis (2004), where black-hole mass $M_{\text{bh}} \propto \text{FWHM}^2$.

With the result that broad-line widths are dependent on spectral index and therefore source orientation, then it is interesting to investigate whether the distribution in broad-line FWHM is due to a disc-like geometry for the broad-line region. Wills & Browne (1986) quantified the broad-line region as comprised of a random isotropic velocity component v_r and a second which is only directed in the plane of a disc v_p . In this scenario, the observed FWHM is given by $\text{FWHM} \simeq 2(v_r^2 + v_p^2 \sin^2 \theta)^{1/2}$, where θ is the angle between the disc normal and the line of sight to the observer. McLure & Dunlop (2002) used a three-parameter model where the intrinsic distribution of orbital velocities in the disc plane is assumed to be Gaussian, with mean V_{orb} and variance σ_{orb}^2 . The third parameter in this model is the maximum opening angle to the line-of-sight, θ_{max} . The distribution in the opening angle is completely random within the solid angle defined between $\theta = 0^\circ \rightarrow \theta_{\text{max}}$, where $\theta = 0^\circ$ represent a source that is pole-on along the line-of-sight.

In Fig. 3 we plot the cumulative distribution in FWHM for the complete sample of radio-quiet quasars from McLure & Jarvis (2004). We enforce a minimum FWHM cut-off of 2000 km s^{-1} to ensure that any incompleteness at these line widths are minimised within the SDSS quasar catalogue⁴. Using the disc model, outlined above, to reproduce the cumulative distribution of the radio-quiet quasars drawn from our sample we find a best fit model with $V_{\text{orb}} = 4700 \text{ km s}^{-1}$, $\sigma_{\text{orb}} = 1800 \text{ km s}^{-1}$ and $\theta_{\text{max}} = 38.5^\circ$. To test whether such a disc model is fair representation of the data we use the 1-D KS-test which shows that the probability of the data being drawn from the best-fit model is 40 per cent. The largest difference between the data and the model occurs at the large FWHMs, where additional processes may alter the distribution. The most relevant of these would be a luminosity dependent torus opening angle, i.e. the receding torus model (Lawrence 1991). However, as the data and model are consistent we do not include more free parameters to include a description of a receding torus model.

Under the assumption that the disc-like model is a fair representation of the true nature of the broad-line regions in quasars, then we are able to constrain the actual difference in orbital velocity for RQQs and RLQs. As we have no reason to believe that the distribution of angles of the disk and the opening angle should be different in RQQs and RLQs, we use the best-fit parameters of σ_{orb} and θ_{max} for the RQQs, and leave V_{orb} as a free parameter to fit the whole RLQ population (both FSQs and SSQs). We find a best-fit of $V_{\text{orb}} = 5950 \text{ km s}^{-1}$ for the RLQs, shown in Fig. 3. The KS-test shows that the probability of the data being drawn from this model is 68 per cent, and is therefore consistent. However, one can immediately see an excess of objects with

$\text{FWHM} < 5000 \text{ km s}^{-1}$ in the RLQ data when compared to the best-fit model distribution.

It is also worth noting that the distribution in FWHM for the RQQs is indistinguishable from that of the FSQs, with the KS-test giving a probability of 75 per cent that they are drawn from the same underlying distribution. On the other hand the KS-test shows that the probability of the SSQs being drawn from the same distribution as the RQQs is $\ll 0.01$ per cent.

We defer discussion of the excess number of RLQ sources at $\text{FWHM} < 5000 \text{ km s}^{-1}$ to the next section, where we also discuss the reason for the agreement between the FWHM distributions of the RQQs and FSQs and their observed difference with the FWHMs of the SSQ broad-lines.

4 DISCUSSION

4.1 Flat-spectrum quasars as beamed radio-quiet quasars

One possible explanation for the similarity in the FWHM distributions for RQQs and FSQs is that the FSQ population is predominantly comprised of RQQs. There is evidence to suggest that radio-quiet quasars have large-scale jets, similar to those found in FRI (Fanaroff & Riley 1974) radio galaxies (Blundell & Rawlings 2001). Due to the orientation of the source, the intrinsic low-luminosity of the radio jet may be Doppler boosted towards the observer. This was discussed fully in Jarvis & McLure (2002) where consideration of both the orientation and Doppler boosting of the radio emission was used to explain the apparent discrepancy of FSQs (Oshlack, Webster & Whiting 2002) on the black-hole mass – radio luminosity correlation put forward by a number of authors (Franceschini, Vercellone & Fabian 1998; Dunlop et al. 2003; McLure et al. 2004).

To estimate the amount of boosting that would be required to place the RQQs in the radio-loud domain at $L_{1.4} > 10^{24} \text{ W Hz}^{-1} \text{ sr}^{-1}$ (Miller, Peacock & Mead 1990), we use the average luminosity of the FSQs, $L_{1.4} = 8.7 \times 10^{25} \text{ W Hz}^{-1} \text{ sr}^{-1}$. In order to boost these sources from the RQQ domain then Doppler factors of $\Gamma^2 \sim 10 - 100$ are required. This is a relatively small amount of boosting. For example, as discussed in Jarvis & McLure (2002) factors of $\sim 100 - 1000$ are easily obtainable under reasonable assumptions of bulk Lorentz factor and, in the case of powerful FSQs, a maximum opening angle of $\theta_{\text{max}} \sim 7^\circ$ (Jackson & Wall 1999). For the larger opening angle of $\theta_{\text{max}} \sim 40^\circ$ from our modelling in section 3.3, then this would obviously reduce the average amount of Doppler boosting⁵. However, a significant fraction of sources would still exhibit substantial amounts of Doppler boosting as they would lie within $\sim 20^\circ$ of our line-of-sight, which may still result in $\Gamma^2 \gtrsim 10$ as the distribution in angles follows $1 - \cos(\theta)$, i.e. proportional to the solid angle. Therefore, given a maximum opening angle of $\theta \sim 40^\circ$ then, for a disc-like broad-line region, we would expect 10 – 25 per cent of the RLQ population to exhibit Doppler factors of $\Gamma^2 > 10$, i.e. those within $\theta < 20^\circ$.

⁴ We note that the formal FWHM limit for the SDSS to classify an object as a quasar is 1000 km s^{-1} .

⁵ The Doppler factor Γ is given by $\Gamma = \gamma^{-1}(1 - \beta \cos \theta)^{-1}$, with $\beta = v/c$, where v the speed of the bulk motion, θ is the angle of the jet to the line of sight, and γ is the bulk Lorentz factor.

Based on this reasoning, as many as half of the FSQs in our sample could be Doppler boosted RQQs. This is qualitatively consistent with Fig. 3 where there is an obvious ridge in the cumulative distribution of RLQs where ~ 20 per cent of the sample deviate from the best fit model at $\lesssim 5000 \text{ km s}^{-1}$.

It is worth noting that the radio-frequency at which the RLQs are selected is the crucial factor which dictates the fraction of flat-spectrum, Doppler boosted sources, in any RLQ sample. For example, the sample used in Oshlack et al. (2002) was derived from the 2.7 GHz Parkes flat-spectrum sample of Drinkwater et al. (1997). Therefore, the Oshlack et al. sample would contain a much higher fraction of Doppler boosted sources than the sample discussed in this paper, due to the fact that by definition it is comprised solely of flat-spectrum sources. Whereas the need for a low-frequency measurement from the WENSS means that the fraction of Doppler boosted sources in our sample is biased towards a lower value. This is due to the fact that many lower luminosity, flat-spectrum radio sources which are detected in FIRST will not be included here as they fall below the WENSS flux-density limit. Therefore, we are enforcing an orientation independent selection on the optical quasars in the SDSS by using the WENSS flux-density limit at 325 MHz.

4.2 Consequences for the virial black-hole mass estimator

In this section we consider how the scenario outlined in section 4.1 would affect the estimation of the black-hole masses in quasars via the virial method (e.g. Wandel, Peterson & Malkan 1999; Kaspi et al. 2000; McLure & Jarvis 2002).

The argument that the FSQs comprise objects that are Doppler boosted from the RQQ regime does fit in with orientation based unified schemes. However, it is important to note that this argument is based on the *average* properties of the FSQ population. Some of them will no doubt be bona fide radio-loud quasars with little or no Doppler boosting, and the fraction of such sources will be heavily dependent on the flux-density limit and frequency of the survey from which the sample is derived, as discussed in section 4.1.

With the disc model for the RQQ and RLQ populations determined in section 3.3, then the difference in black-hole mass of RQQs and RLQs is 0.18 dex (as $M_{\text{bh}} \propto V_{\text{orb}}^2$), consistent with the 0.16 dex found by assuming $\text{FWHM} \equiv V_{\text{orb}}$ in the analysis of McLure & Jarvis (2004), where no consideration of source orientation was made. The sample of RLQs used in McLure & Jarvis comprised all of the radio sources with detections in FIRST, without the need for a WENSS detection, thus it is highly likely that the fraction of flat-spectrum sources is larger in the complete sample. Unfortunately this is currently impossible to test due to the lack of low-frequency radio data for all of the sources. Moreover, if higher-resolution, multi-frequency radio data were available for the sample used here then it is likely that the difference in black-hole mass for the RQQs and genuine RLQs would increase as the beamed RQQs could be removed from the RLQ sample. This would then push the difference closer to the value found from modelling of the host galaxies of radio galaxies and quasars. At low redshift ($0.1 < z < 0.25$), Dunlop et al. (2003) showed that the black-hole masses derived using the relation between black-hole mass and spheroid lu-

minosity (e.g. Magorrian et al. 1998; Gebhardt et al. 2000; Merritt & Ferrarese 2001) were significantly lower in radio-quiet quasars, with a mean difference of ~ 0.22 dex. The radio luminosity dependence on black-hole mass is also consistent with results from modelling the host galaxies of powerful radio galaxies. Using the black-hole mass – bulge luminosity relation to estimate black-hole mass, McLure et al. (2004) showed that the radio luminosity of powerful FRII-type (Fanaroff & Riley 1974) radio galaxies is correlated with the bulge luminosity and hence the black-hole mass, at least at $z \sim 0.5$.

Therefore, our analysis reinforces the view that *intrinsic* radio power is dependent on the black-hole mass. However, there will be a coupling with extra parameters such as accretion rate and/or black-hole spin, along with the orientation effects discussed here.

This can also be seen in the principal component analysis (PCA) of Boroson (2002). The median value for principal component 1, which is believed to represent the accretion rate, for FSQs is shifted closer to the region in which the RQQs lie when compared to the SSQs. This implies that, even in these radio-selected samples, FSQs and RQQs may be drawn from the same population within ~ 1 dex of the boundary of radio-loud and radio-quiet classification. Unfortunately, we do not have enough sources in our sample at the correct redshift to carry out the PCA discussed in Boroson (2002). However deeper low-frequency radio observations of the quasars over the FIRST area would allow us to increase the sample size at low redshift and thus carry out the PCA.

We have shown that the FWHM of broad lines measured in both the RLQs and the RQQs will have an orientation dependency. Therefore, measuring black-hole masses via the virial estimate on small samples may lead to spurious results. However, the scatter due to the source orientation should be overcome if large samples of quasars are used, and this is evidently possible with quasar surveys such as the SDSS and 2dfQSO (Croom et al. 2004).

Decoupling orientation effects and black-hole mass differences will be a difficult task. However, deep high-resolution multi-frequency radio observations of large samples of RQQs will provide the best way of placing direct constraints on this problem.

5 SUMMARY

We have used our well defined sample of radio-loud and radio-quiet quasars to investigate the dependence of the observed broad-line widths on orientation. To summarise

- Radio-quiet quasars and the flat-spectrum quasars exhibit the same distribution in broad-line widths, whereas the steep-spectrum population exhibit a distribution which is shifted significantly to broader widths.
- The difference in FWHM distributions can be explained within unified schemes where a substantial fraction of the flat-spectrum sources are composed of Doppler boosted radio-quiet quasars. For the sample we use in this paper, this fraction could be as high as 50 per cent of the flat-spectrum quasars and 25 per cent of all radio-loud quasars.
- In light of this we agree with previous results which suggest that radio-quiet quasars contain less massive black holes than their radio-loud quasar counterparts. We find a

difference on the mean black-hole masses of 0.18 dex between radio-loud and radio quiet quasars. However, this is likely to be a lower limit due to the difficulty in accounting for beamed radio-quiet quasars which lie above the divide which separates radio-loud and radio-quiet quasars.

- Under this hypothesis, the measured broad-line widths are dependent on both orientation and black-hole mass. The level of orientation bias will be heavily dependent on the selection method, thus studies using the black-hole masses derived from the virial estimate need well defined quasar samples where any possible orientation bias is kept to a minimum.

- We suggest that a method of decoupling the dependencies of orientation and black-hole mass and to keep orientation effects to a minimum would be to carry out deeper low-frequency radio observation across the FIRST area covered by the SDSS. Such a survey could be easily achieved with future radio telescopes such as the low-frequency array (LOFAR; <http://www.lofar.org>).

ACKNOWLEDGEMENTS

MJJ acknowledges funding from a PPARC PDRA and RJM acknowledges funding from the Royal Society. We thank the referee Katherine Inskip for a detailed reading of the manuscript. This publication makes use of the material provided in the FIRST, NVSS and SDSS surveys. FIRST is funded by the National Radio Astronomy Observatory (NRAO), and is a research facility of the US National Science foundation and uses the NRAO Very Large Array. Funding for the creation and distribution of the SDSS Archive has been provided by the Alfred P. Sloan Foundation, the Participating Institutions, the National Aeronautics and Space Administration, the National Science Foundation, the U.S. Department of Energy, the Japanese Monbukagakusho, and the Max Planck Society. The SDSS Web site is <http://www.sdss.org/>. The SDSS is managed by the Astrophysical Research Consortium (ARC) for the Participating Institutions. The Participating Institutions are The University of Chicago, Fermilab, the Institute for Advanced Study, the Japan Participation Group, The Johns Hopkins University, the Korean Scientist Group, Los Alamos National Laboratory, the Max-Planck-Institute for Astronomy (MPIA), the Max-Planck-Institute for Astrophysics (MPA), New Mexico State University, University of Pittsburgh, University of Portsmouth, Princeton University, the United States Naval Observatory, and the University of Washington.

REFERENCES

Antonucci R., 1993, *ARA&A*, 31, 473
 Barthel P.D., 1989, *ApJ*, 336, 606
 Becker R.H., White R.I., Helfand D.J., 1995, *ApJ*, 450, 559
 Blundell K.M., Rawlings S., 2001, *ApJ*, 562, 5
 Boroson T.A., 2002, *ApJ*, 565, 78
 Brotherton M.S., 1996, *ApJS*, 102, 1
 Condon J.J., Cotton W.D., Greisen E.W., Yin Q.F., Perley R.A., Taylor G.B., Broderick J.J., 1998, *AJ*, 115, 1693
 Croom S.M., Smith R.J., Boyle B.J., Shanks T., Miller L., Oram P.J., Loaring N.S., 2004, *MNRAS*, 349, 1397

Drinkwater M.J., Webster R.L., Francis P.J., Condon J.J., Ellison S.L., Jauncey D.L., Lovell J., Peterson B.A., Savage A., 1997, *MNRAS*, 284, 85
 Dunlop J.S., McLure R.J., Kukula M.J., Baum S.A., O’Dea C.P., Hughes D.H., 2003, *MNRAS*, 340, 1095
 Eales S., Rawlings S., Law-Green D., Cotter G., Lacy M., 1997, *MNRAS*, 291, 593
 Fanaroff B.L., Riley J.M., 1974, *MNRAS*, 167, 31
 Franceschini A., Vercellone S., Fabian A.C., 1998, *MNRAS*, 297, 817
 Gebhardt K., et al., 2000, *ApJ*, 539, L13
 Hine R.G., Scheuer P.A.G., 1980, *MNRAS*, 193, 285
 Hough D.H., Readhead A.C.S., 1989, *AJ*, 98, 1208
 Jackson C.A., Wall J.V., 1999, *MNRAS*, 304, 160
 Inskip K.J., Best P.N., Rawlings S., Longair M.S., Cotter G., Röttgering H.J.A., Eales S., 2002, *MNRAS*, 337, 1381
 Jarvis M.J., McLure R.J., 2002, *MNRAS*, 336, L38
 Kaspi S., Smith P.S., Netzer H., Maoz D., Jannuzi B.T., Givon U., 2000, *ApJ*, 533, 677
 Laing R.A., Riley J.M., Longair M.S., 1983, *MNRAS*, 204, 151
 Lawrence A., 1991, *MNRAS*, 252, 586
 Magorrian J., et al., 1998, *AJ*, 115, 2285
 McLure R.J. & Dunlop J.S., 2002, *MNRAS*, 331, 795
 McLure R.J. & Dunlop J.S., 2004, *MNRAS*, 352, 1390
 McLure R.J. & Jarvis M.J., 2002, *MNRAS*, 337, 109
 McLure R.J. & Jarvis M.J., 2004, *MNRAS*, 353, 45
 McLure R.J., Willott C.J., Jarvis M.J., Rawlings S., Hill G.J., Mitchell E., Dunlop J.S., Wold M., 2004, *MNRAS*, 351, 347
 Merritt D., Ferrarese L., 2001, *MNRAS*, 320, 30
 Miller L., Peacock J.A., Mead A.R.G., 1990, *MNRAS*, 244, 207
 Orr M.J.L., Browne I.W.A., 1982, *MNRAS*, 198, 673
 Oshlack A.Y.K.N., Webster R.L., Whiting M.T., 2002, *ApJ*, 576, 81
 Peacock J.A., 1983, *MNRAS*, 202, 615
 Rengelink, R.B., et al., 1997, *AAPS*, 124, 259
 Schneider D.P., et al., 2003, *AJ*, 126, 2579
 Urry C.M., Padovani P., 1995, *PASP*, 107, 803
 van Breugel W., Heckman T., Miley G., 1984, *ApJ*, 276, 79
 Vestergaard M., 2002, *ApJ*, 571, 733
 Wandel A., Peterson B.M., Malkan M.A., 1999, *ApJ*, 526, 579
 Willott C.J., Rawlings S., Blundell K.M., Lacy M., Hill G.J., Scott S.E., 2002, *MNRAS*, 335, 1120
 Wills B.J., Browne I.W.A., 1986, *ApJ*, 302, 56